The effect of containing Al_2O_3 microparticles in different matrix polymers on properties of pineapple fiber-reinforced composites

Indra Mawardi, Hanif Razak, Zaini Akadir
Department of Mechanical Engineering, Politeknik Negeri Lhokseumawe, Lhokseumawe, 24301, Indonesia
indratm@pnl.ac.id, http://orcid.org/0000-0001-6631-510X
hanifrazak63@gmail.com, zainiak4@gmail.com

Ramadhansyah Putra Jaya
Faculty of Civil Engineering Technology, Universiti Malaysia Pahang Al-Sultan Abdullah, 26300 Kuantan, Pahang, Malaysia
ramadhansyah@ump.edu.my, http://orcid.org/0000-0002-5255-9856

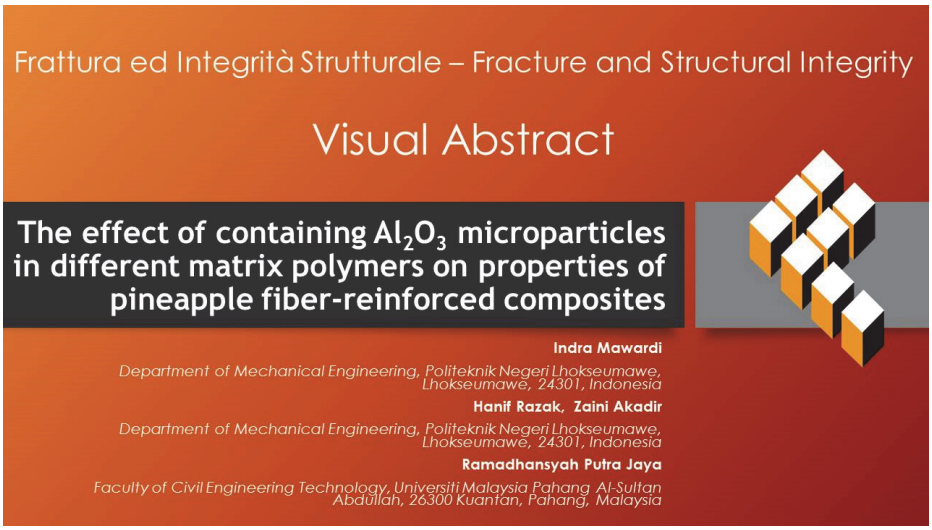

Citation: Mawardi, I., Razak, H., Akadir, Z., Jaya, R.P, The effect of containing Al_2O_3 microparticles in different matrix polymers on properties of pineapple fiber-reinforced composites, Frattura ed Integrità Strutturale, 67 (2024) 94-107.

Received: 14.07.2023
Accepted: 28.10.2023
Online first: 31.10.2023
Published: 01.01.2024

KEYWORDS. Pineapple fiber, Composite, Alumina, Epoxy, Unsaturated Polyester.

INTRODUCTION

Natural-fiber-reinforced composites, or "green composites," have been the subject of extensive investigations in recent years for use in a variety of structural and non-structural applications. They are considered a preferable alternative to synthetic fibers due to their biodegradable, sustainable, and economical properties as opposed to synthetic fibers, which are known to be environmentally harmful, non-renewable, and difficult to decompose, leading to increased carbon dioxide and greenhouse gas emissions [1,2]. One natural fiber that has the potential to replace synthetic fibers is the pineapple leaf fiber (PALF). Because of its ability to biodegrade, this fiber has minimal environmental effects.

PALF has gained significant attention as a reinforcement in polymeric composites, in addition to other fibers such as coir, sisal, hemp, flax, and kenaf. PALF is a natural fiber derived from the pineapple plant (*Ananas comosus*), which belongs to the Bromeliaceae family. PALF is extracted from pineapple leaves. It consists of 70–82% cellulose, 13.6–21% hemicellulose, 5–12% lignin, and 1.1% pectin [3]. It is abundant in tropical climates, particularly in Southeast Asian nations, such as Thailand, Malaysia, the Philippines, and Indonesia [3,4]. Today, world pineapple production is around 33.38 million tons per year, of which Indonesia produces 2.45 million tons [5]. PALF has been developed for various applications, such as infrastructure, packaging, biomedicine, furniture, automotive, etc. It exhibits good mechanical properties and is environmentally friendly, making it a widely used reinforcing material in polymer composites [6].

However, natural fibers such as PALF have several limitations, including hydrophilic properties, variable and irregular fiber dimensions, and relatively low fiber properties compared to synthetic fibers. One technique to overcome this problem is to modify the matrix using micro- and nanofillers. Fillers play an important role in helping to increase the wettability and interface of the base material so that, in the end, they affect the final properties of the composite. Mishra et al. [3] suggested another method to improve the performance of natural composites, that is, to use particulate fillers such as alumina (Al_2O_3), silicon, graphite, and carbon. The incorporation of fillers into the composite improves the rigidity of the matrix phase and the cross-linkage between the matrix and the reinforcement, such that the physical, mechanical, heat resistance, and wear resistance properties of the composite become enhanced. The dispersal of fillers can also cover microvoids, which slows crack propagation and failure [7].

In addition to the types of reinforcement and filler, the type of polymer matrix also influences the characteristics of the composite. The matrix selection is based on the application requirements of the composite materials. Epoxy and unsaturated polyester resins (UPRs) are two widely used thermoset matrices for various structural and performance applications. Both resins have low cost, low density, good chemical resistance, and excellent processability [8]. Mishra et al. [3] investigated the characteristics and potential industrial applications of hybrid composites filled with inorganic nanoparticles. The effect of adding inorganic fillers to unreinforced polymer composites on water uptake, thermal conductivity, and tensile strength has been investigated. All the three properties examined showed positive results with the inclusion of a filler in the composite matrix [9]. The incorporation of SiC, graphene, Al_2O_3, and titanium oxide fillers in polyester and epoxy polymer composites reinforced with a natural fiber also affects the mechanical and physical properties [10]. In addition, the influence of inorganic fillers on natural fiber composites (e.g., flax [11], sisal [12], coir and banana [13], and jute and hemp) has also been examined [14].

Numerous works have studied the effect of inorganic fillers as composite fillers. However, studies on the impact of adding the alumina filler on the physical and mechanical properties of PALF-reinforced composites have yet to be conducted. Radoor et al. [15] examined the technique for the extraction of PALF and PALF use as reinforcement in polymer matrices. Other studies have also investigated the suitability, competitiveness, and capacity of PALF as a reinforcement in natural composites [16,17]. The mechanical and physical properties of PALF-reinforced polymer composites are influenced by aspects such as aspect ratio, microfibrillar angle, crystallinity, and cellulose concentration, similar to other natural fibers. Potluri et al. [18] figured out that adding the Al_2O_3 filler enhances the water absorption, wear resistance, and strength of pineapple leaf, sisal, and coir fiber hybrid composites.

Although many research studies have been published on the characteristics of polymeric composites with the incorporation of inorganic fillers, studies investigating the impact of Al_2O_3 microparticles on the properties of PALF-reinforced epoxy and UPRs composites have yet to be published. Therefore, this study aims to investigate the effect of Al_2O_3 microparticles addition to PALF-reinforced polymeric composites (with epoxy and UPRs matrices) on the physical, mechanical, and thermal properties of the composites. The composites were manufactured by the hand lay-up technique with 30 wt% pineapple fiber and a fiber orientation of 0 degrees.

MATERIALS AND METHODS

Materials

The PALF-reinforced composites were manufactured using epoxy and UPRs matrices with variable levels of Al_2O_3 microparticle content. PALF was collected from Subang, West Java, Indonesia. The Al_2O_3 microparticles, purchased from Labchem Sdn. Bhd, Selangor, Malaysia, were used as a filler in powdered form (50–90 μm) with a purity level > 99.9%. In this study, two types of matrix, epoxy and UPRs, were provided by Justus Kimia Raya, Medan, Indonesia. The epoxy matrix consisted of bisphenol A diglycidyl ether (Eposchon A) and polyaminoamide (Eposchon B) as a hardener in a 1:1 ratio. Meanwhile, the UPRs matrix (Yukalac 157 BQTN-EX) was hardened with 1% methyl ethyl

ketone peroxide. The various characteristics of PALF, Al_2O_3, and the matrices are shown in Tab. 1. The PALF-reinforced composites' forming materials are shown in Fig. 1.

Chemical/Properties	Pineapple [15,19]	Al_2O_3 [20],[21]	Epoxy [22]	UPRs [20]
Cellulose (%)	70-82	-	-	-
Hemicellulose (%)	19.5	-	-	-
Lignin (%)	5-12	-	-	-
Density (g/cm^3)	0.8-1.6	3.78-3.95	1.13	1.09-1.35
Tensile strength (MPa)	184-627	200-265	26.84	40
Young's modulus (GPa)	1.44-6.32	210-380	2-6	3.33
Poisson ratio	-	0.24-0.30	0.20-0.35	0.44

Table 1: The chemical content and mechanical and physical properties of the composites' raw materials

Figure 1: PALF and Al_2O_3 microparticle filler materials

Two types of PALF-reinforced composite structures were produced, as shown in Tab. 2. The PALF-reinforced composite structures consisted of epoxy and UPRs matrices mixed with Al_2O_3 at 0, 5, 10, and 15 wt%.

Type of specimen	Epoxy (wt.%)	UPRs (wt.%)	Pineapple fiber (%)	Al_2O_3 (wt.%)
CE0	70	0	30	0
CE5	65	0	30	5
CE10	60	0	30	10
CE15	55	0	30	15
CP0	0	70	30	0
CP5	0	65	30	5
CP10	0	60	30	10
CP15	0	55	30	15

Table 2: The structure design of PALF-reinforced composites with Al_2O_3 microparticles

Composites production process

In this study, the first process carried out was the selection of fiber dimensions. The PALF obtained was cleaned with water and then dried in an oven (Memmert Oven model UN55 53L, Germany) until it reached a moisture content of 10–15% before being used. This study used PALF with a weight fraction of 30% as a continuous phase (0° fiber orientation) and 0, 5, 10, and 15 wt% of Al_2O_3 to prepare the composites. A mold was prepared from a blockboard with dimensions of 300 × 250 × 15 mm. The mold was covered with aluminum foil, and PALF was placed on it. Aluminum foil was used for easy removal of the composite from the mold.

Composites were made using the hand lay-up technique. Direct mixing was applied to create both types of composites. Homogenous dispersion was first achieved by adding Al_2O_3 powder to the resin and stirring with a mechanical stirrer (mixer model HM-620 Miyako, Japan) at 200 rpm for 3 minutes. Catalysts or hardeners were used as initiators for curing processes. After complete mixing, the finished mixture was poured into the mold, followed by rolling and a 24-hour curing process before the mixture was removed from the mold. For each experimental scenario, five samples were created and checked in accordance with ASTM standards. The composites were cured at room temperature for seven days before testing. Fig. 2 depicts the stages of manufacturing the PALF-reinforced composite specimens with the alumina filler.

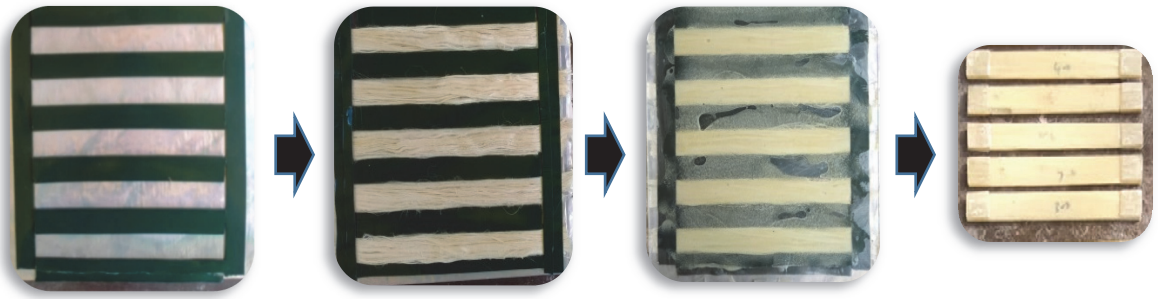

Figure 2: The manufacturing of PALF-reinforced composites with the alumina filler

Characterization of composites

The effect of Al_2O_3 microparticles in the PALF-reinforced composites was evaluated by carrying out physical and mechanical tests on the prepared samples.

Physical characterization

Physical characterization tests consisted of density and water absorption tests. The density test of the PALF-reinforced composites used the theorem of Archimedes using water as a medium and precision scales (model AND EK-610i Compact Balance, Japan) in reference to the ASTM D792 standard [23]. Five specimens were prepared according to the experimental design, and averages were calculated to determine the composite density for each level of Al_2O_3 content. To evaluate the water absorption performance of the composites, the ASTM D570 [24] standard was used. Samples with dimensions of 25 × 25 × 3 mm were dried in an oven before being immersed in water for 16 days. Every 2 days, the samples were taken out and weighed again, and the dry weight after immersion was recorded.

Mechanical characterization

The investigation of mechanical properties consisted of tensile strength, flexural strength, and shore hardness tests. PALF-reinforced composite samples were prepared for tensile (230 × 25 × 3 mm) and flexural strength (100 × 25 × 3 mm) tests according to the ASTM D3039 [25] and ASTM D790 standards [26], respectively. An RTF 1350 model Tensilon universal testing machine (Japan) with a 50 kN load cell was used in both tests at 5 mm/min and 2 mm/min crosshead speed for the tensile and flexural strengths, respectively. The flexural strength of the PALF-reinforced composite samples was evaluated using the three-point method. Furthermore, a composite hardness test was carried out using a 0.5 HD Shore D digital durometer (China) in accordance with the ASTM D2240 standard [27]. Hardness was evaluated by inserting a durometer needle into the composite samples and reading the resulting hardness numbers on the pointer. Measurements were taken on both sides by calculating the average of five readings.

Thermogravimetric analysis

The influence of different matrices and fillers on the thermal degradation characteristics of the PALF-reinforced composites was investigated using the Thermogravimetric Analysis (TGA) test. TGA tests were carried out using a thermal analyzer (SHIMADZU DTG 60, Japan) following the ASTM E1131-08 standard [28]. A sample of 5 mg was

heated in a sample pan from 30 °C to 600 °C in a nitrogen atmosphere at a heating rate of 40 °C/min, with a flow rate of 20 ml/min. In general, the research flowchart diagram is shown in Fig. 3.

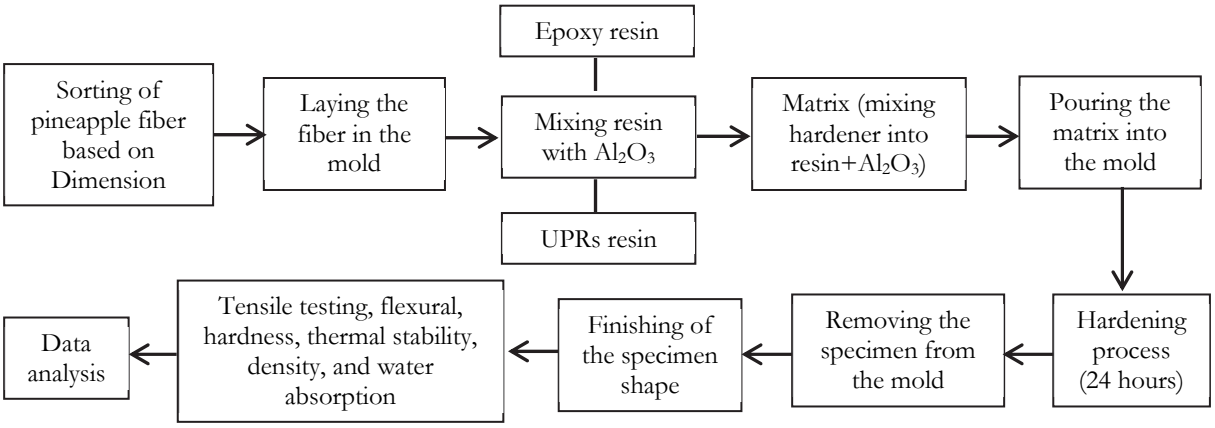

Figure 3: Research flowchart diagram

Results and Discussion

Characterization of the mechanical and physical properties, as well as the thermal stability, showed a variety of composite performance depending on the amount of Al_2O_3 filler and the type of matrix used. The following are some of the findings from the characterization tests.

Effect of Al_2O_3 contents on tensile strength

The tensile property is one of the most crucial mechanical characteristics of a material. This stress is the external force required to break the sample and is usually found at the peak of the stress-strain curve. Fig. 4a–b illustrates the stress-strain curves from the tensile tests of the PALF-reinforced epoxy and UPRs composites with Al_2O_3 filler. As shown in Fig. 4a, all PALF-reinforced epoxy composites with the Al_2O_3 filler show lower stiffness than the composites without filler. The same held true with the UPRs composites (Fig. 4b), but these composites had lower stress than the epoxy composites. Fig. 4 and Tab. 3 show some of the composites' mechanical properties.

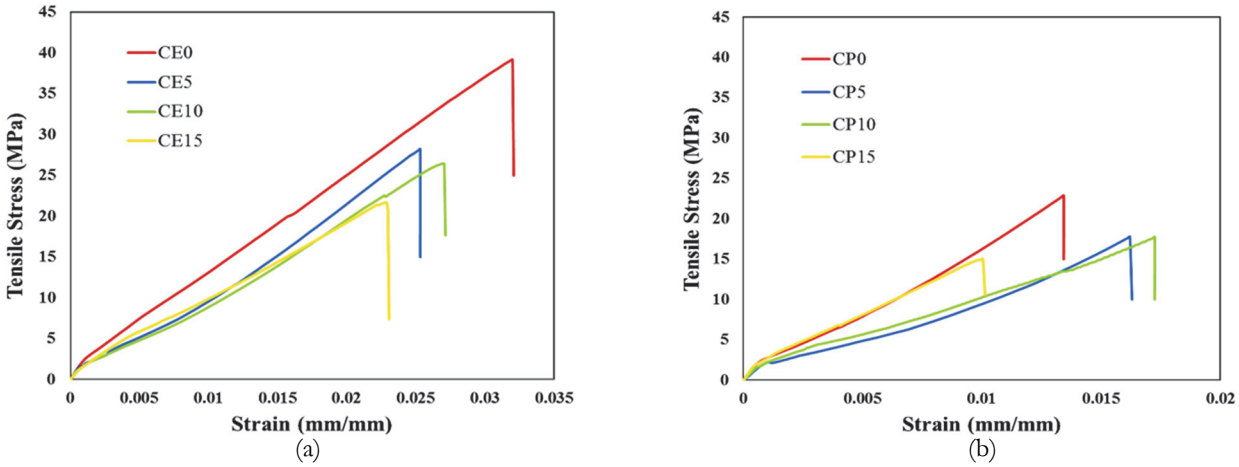

Figure 4: Stress-strain curves of tensile properties of the PALF/Al_2O_3 composites: epoxy matrix, (b) UPRs matrix.

The tensile and flexural strengths of the PALF-reinforced epoxy and UPRs composites at varying concentrations of Al_2O_3 microparticle filler are shown in Tab. 3. This table also shows the corresponding tensile and flexural results of the epoxy and UPRs composites without filler as control specimens. Fig. 5 depicts the results from Tab. 3 for visual interpretation. It is shown in the figure that the epoxy composites had greater tensile strength than the UPRs composites.

The tensile strength of the PALF-reinforced epoxy and UPRs composites ranged from 22.42 MPa to 33.54 MPa and from 15.39 MPa to 21.62 MPa, respectively. In addition, the PALF-reinforced epoxy and UPRs composites with 0% filler (CE0 and CP0) displayed tensile strength values superior to the PALF-reinforced epoxy and UPRs composites with 15 wt% Al_2O_3 (CE15 and CP15). In this case, the presence of more Al_2O_3 microparticles could gradually reduce the tensile strength. Compared to the decrease of tensile strength of the composites without Al_2O_3 (i.e., 33.54 MPa), the epoxy composites with 5, 10, and 15 wt% Al_2O_3 filler decreased in tensile strength by 16.70, 24.92, and 49.59%, respectively. For the UPRs composites, the decreases in tensile strength ranged from 19.51 to 40.48%. The decrease in tensile strength might be due to agglomerations that acted as stress concentration centers representing internal defects. This caused weakening and ultimately decreased the tensile strength [29–31]. Fig. 6 shows the scanning electron microscopy (SEM) images of composite defects, where alumina microparticle agglomerations caused poor interfacial interaction between the fiber and filler and the matrix, which caused a decrease in tensile strength. In addition to agglomerations, composites have micro-defects as voids that initiate cracks. Moreover, as revealed by previous studies involving nanofillers addition, tensile strength tends to decrease with increasing Al_2O_3 content in the polymer matrix [32].

Samples	Tensile strength (MPa)	Flexural strength (MPa)
CE0	33.54 ± 2.9	26.88 ± 4.3
CE5	28.74 ± 2.5	38.61 ± 3.7
CE10	26.85 ± 2.6	39.92 ± 3.6
CE15	22.42 ± 2.2	47.58 ± 3.5
CP0	21.62 ± 2.7	62.22 ± 3.8
CP5	18.09 ± 2.1	72.21 ± 3.6
CP10	17.24 ± 2.4	73.97 ± 3.8
CP15	15.39 ± 2.3	86.20 ± 4.1

Table 3: Mechanical characteristics of the PALF/Al_2O_3 composites.

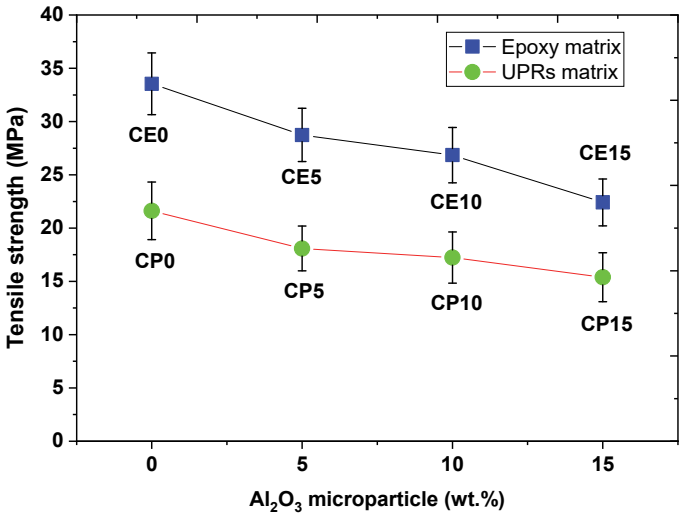

Figure 5: Comparison of tensile strength of the PALF/Al_2O_3 composites using epoxy and UPRs matrices.

Effect of Al_2O_3 contents on flexural strength

The stress-strain curves for the flexural test are similar to the stress-strain curves for the tensile test, but the strain that occurred in the former was longer than the strain that occurred in the latter. As observed in Fig. 7, the strain-break of the composites increased with increasing Al_2O_3 content. The elongation was directly comparable to the flexural strength. An increase in flexural strength usually leads to an increase in strain.

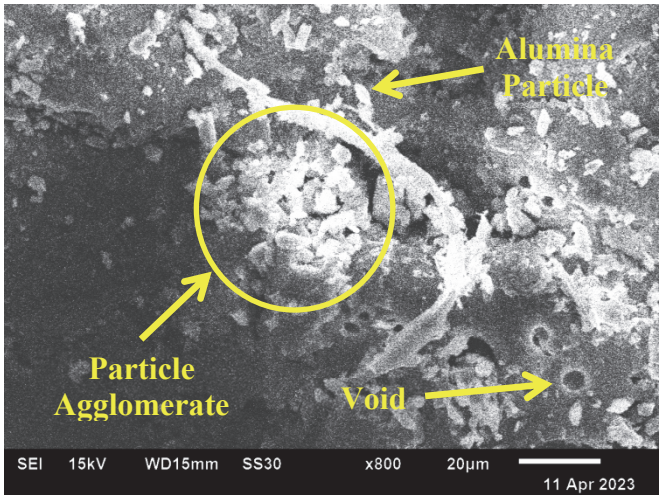

Figure 6: SEM images of Al_2O_3-filled PALF-reinforced composites.

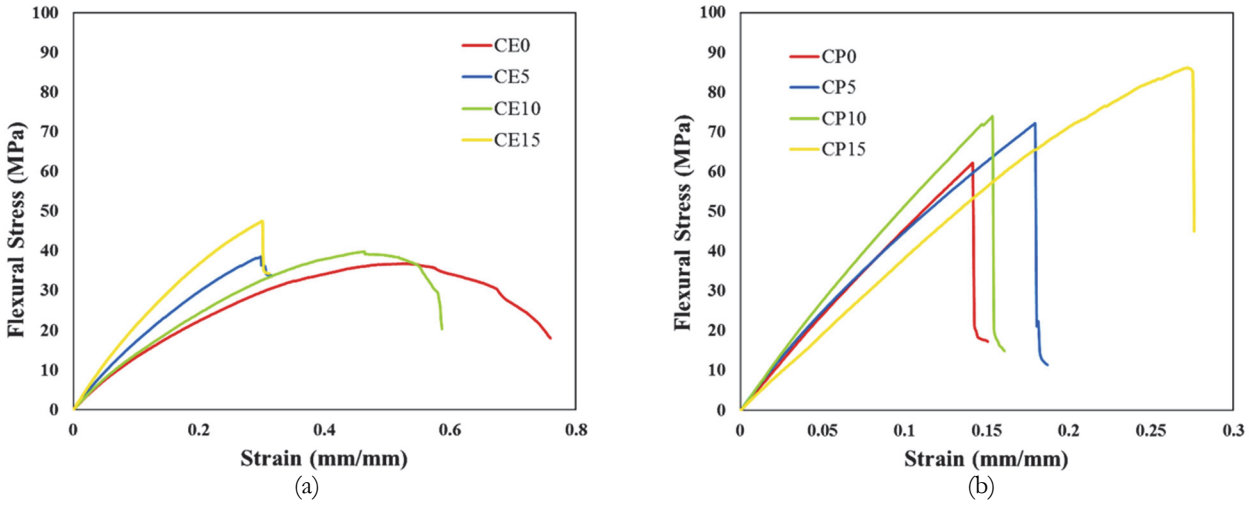

Figure 7: Stress-strain curves of the flexural property for the PALF/Al_2O_3 composites. (a) epoxy matrix, (b) UPRs matrix

Fig. 8 depicts that the flexural strength of the PALF-reinforced epoxy and UPRs composites was affected by Al_2O_3 incorporation. The flexural strength of the composites with the UPRs matrix was higher than that of the composites with the epoxy matrix (~45.67%). The flexural strength of the epoxy and UPRs composites ranged from 26.88 MPa to 47.58 MPa and from 62.22 MPa to 86.20 MPa, respectively. Furthermore, the composites with 15 wt% Al_2O_3 microparticles (CP15 and CE15) had the maximum flexural strength. The composites' flexural strength gradually increased as the percentage of Al_2O_3 microparticles increased.

The increases in flexural strength of the filler-incorporated PALF-reinforced composites might be attributed to polymeric chain interlocking due to Al_2O_3 microparticles (Fig. 9). The composites could better resist external pressure, which increased the flexural strength. In addition, the flexural strength was also influenced by the properties of Al_2O_3 microparticles. This finding helps devise a strategy to improve the flexural strength of composite materials. Similar findings were also observed in previous studies with the incorporation of different fillers in polymer composites [33,34].

Effect of Al_2O_3 contents on hardness

Tab. 4 shows the PALF-reinforced composites' Shore D hardness observed with different matrices and Al_2O_3 loadings. The Shore D hardness of the composite specimens with both matrices increased with the increase in Al_2O_3 filler content.

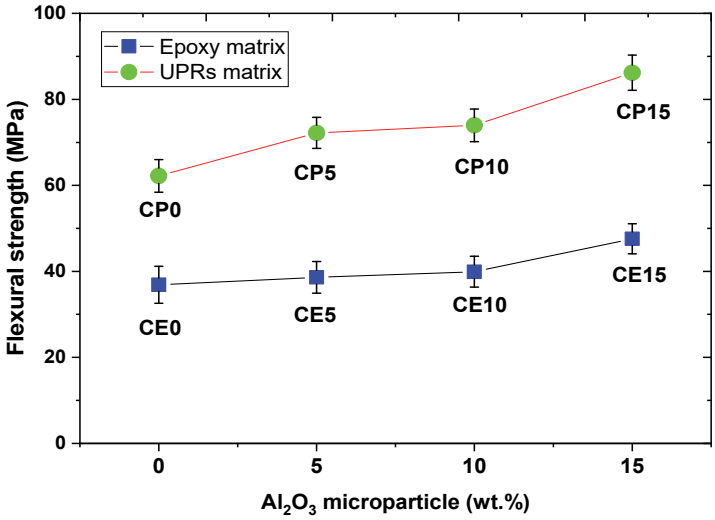

Figure 8: Comparison of flexural strength of the PALF/Al_2O_3 epoxy and UPRs composites

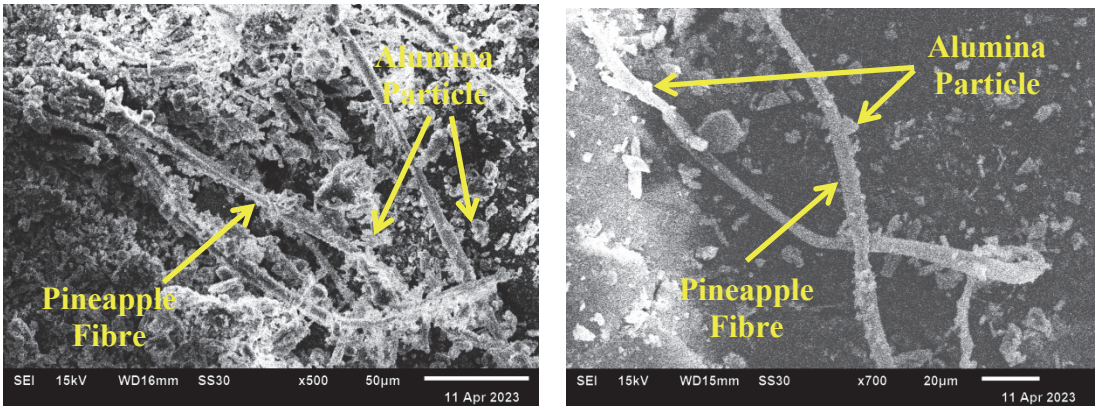

Figure 9: Surface micrographs of PALF-reinforced composites with alumina microparticles

Sample	CE0	CE5	CE10	CE15
Shore-D hardness	61.6 ± 2.12	63.2 ± 1.84	64.5 ± 2.62	66.8 ± 3.25
Sample	CP0	CP5	CP10	CP15
Shore-D hardness	58.2 ± 2.21	62.6 ± 2.16	72.2 ± 2.82	81.5 ± 2.54

Table 4: PALF/alumina composites' Shore D hardness

For the PALF-reinforced epoxy composite with 0% filler, the Shore D hardness value was 61.6, whereas the maximum increase was obtained by the composite filled with 15 wt% Al_2O_3 microparticles (CE15). This Shore D hardness measured 66.8 at the maximum, which was approximately 8.4% higher than the Shore D hardness value obtained by the 0-wt%-Al_2O_3-filled composite (CE0). It can also be observed from Tab. 3 that the UPRs composites filled with Al_2O_3 microparticles had the maximum shore D hardness value of 81.5 (CP15 sample). In the case of composites filled with 10 and 15 wt% Al_2O_3, the Shore D hardness of the UPRs composites was higher than that of the epoxy composites.

In general, the addition of Al_2O_3 to the composites enhanced the composite hardness. The hard Al_2O_3 microparticles blocked the movement of the polymeric bonds. Consequently, the composites became more resistant to external indentation, leading to higher hardness values [35]. The homogeneous distribution of filler particles could cover voids, which leads to increased indentation resistance. However, the increase in the filler content in the composite also triggers

an increase in the risk of agglomeration. In this work, agglomeration has a negative effect on tensile strength, but a positive effect on flexural strength (Fig. 10).

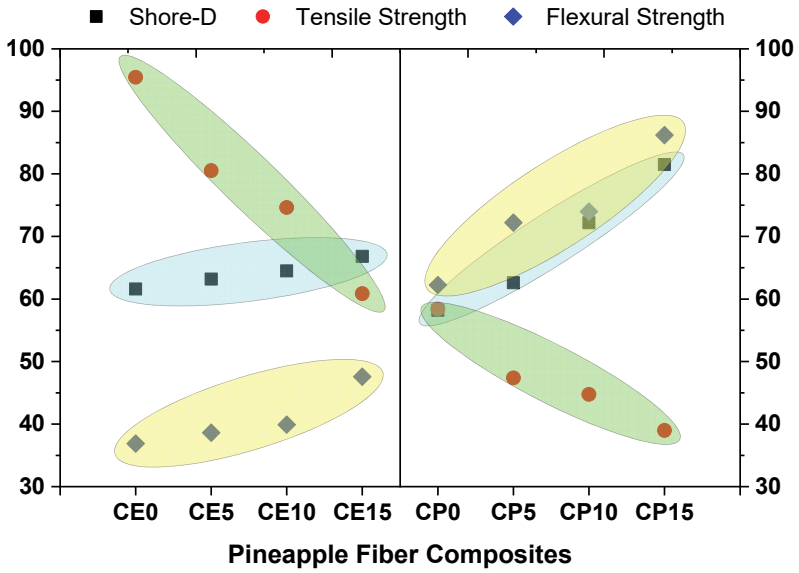

Figure 10: The correlation of Shore D hardness with the tensile and flexural strengths of Al_2O_3-filled PALF-reinforced composites

Several researchers have previously published that the incorporation of nano-Al_2O_3 improves hybrid composites' mechanical properties and wear behavior [34]. Nayak et al. and Latief et al., for instance, reported an increase in the hardness of UPRs composites filled with marble dust and micro-Al_2O_3 [10,36]. The Shore D hardness of the PALF-reinforced UPRs composites was higher than that of the PALF-reinforced epoxy composites. This suggests that the matrix used also has a role in determining the hardness of a composite. In this study, the composites produced were categorized as hard, for CP0, and extra hard, for the other samples [37] (Fig. 11).

Figure 11: The PALF-reinforced composites' positions in terms of Shore D hardness category

Effect of Al_2O_3 contents on physical properties

Fig. 12 shows the graphical depiction of the theoretical and experimental densities of the PALF-reinforced epoxy and composites with different levels of Al_2O_3 content. For all samples, the theoretical density was slightly higher than the UPRs experimental density. This finding can be attributed to the voids in the composites that formed due to the production process being carried out by hand lay-up. Therefore, forming composites in a vacuum is highly recommended to reduce voids [10,36]. The experimental density of the epoxy and UPRs composites ranged from 1.11 to 1.23 g/cm³ and from 1.18 to 1.36 g/cm³, respectively. When the Al_2O_3 filler was added, the value of density increased, which was the highest for the composite with 15 wt% Al_2O_3 microparticles. The effect of Al_2O_3 on density was higher than that of the other constituents of the composite, which improved the average density of the PALF-reinforced composite as a whole.

Fig. 13 shows the effect of Al_2O_3 microparticles on the water absorption behavior of the PALF-reinforced epoxy and UPRs composites. The water absorption performance of all composite samples was significant from the second to the twelfth day and became practically constant until the sixteenth day. The results showed that all samples experienced an increase in their water-holding capacity over a long time until they were saturated on the twelfth day. In this case, the

UPRs composites performed better in terms of water resistance than the epoxy composites. The different physical properties of both matrices led to differences in water absorption performance. The UPRs matrix has more excellent density than the epoxy matrix, so the UPRs composites had better water resistance than the epoxy composites. Furthermore, the water absorption capacity of the epoxy and UPRs composites ranged from 2.94 to 8.47% and from 2.56 to 3.85%, respectively, in which case the CE0 and CP0 samples had the highest water absorption performance.

PALF is hydrophilic and tends to absorb moisture when exposed to water. This may cause the fiber to swell and create microcracks at the matrix-fiber interface, thereby affecting the mechanical properties of the composite. Adding the alumina filler into the matrix gradually reduces the water absorption ability of natural fiber composites. The hydrophobic alumina filler reduces a PALF-reinforced composite's water intake affinity and covers microcracks or cavities trapped in the composite [14].

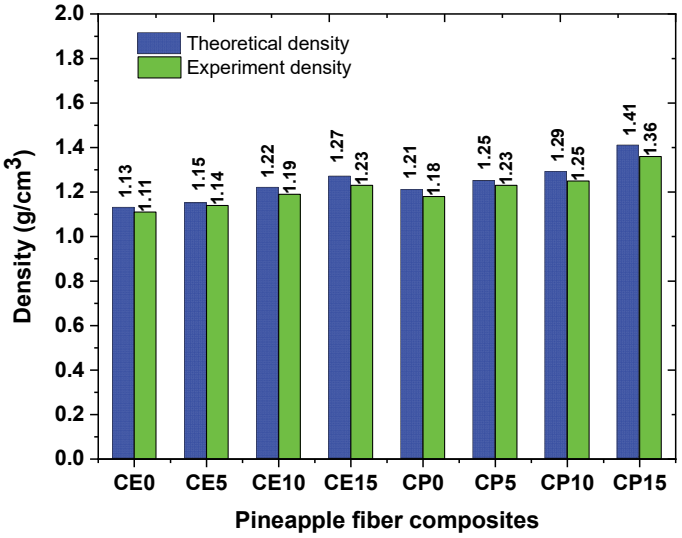

Figure 12: Graph of the experimental and theoretical densities of the Al_2O_3-filled PALF-reinforced composites

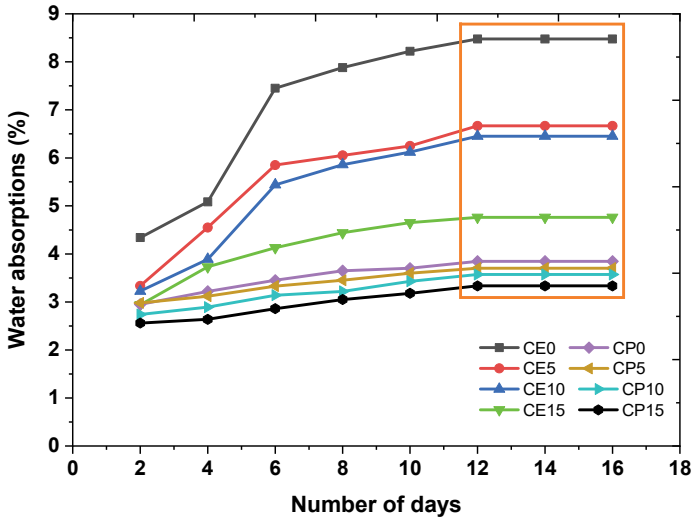

Figure 13: The water absorption performance of the Al_2O_3-filled PALF-reinforced composites.

Effect of Al_2O_3 contents on thermal stability

Fig. 14 shows the TGA curves of the Al_2O_3-filled PALF-reinforced epoxy and UPRs composites. The composites with the two different matrices showed similar decomposition patterns with three phases of mass loss. The first phase of mass loss due to moisture evaporation occurred at 30–152 °C at about 4.4% and 30–156 °C at about 3.6% for epoxy and UPRs composites, respectively. The mass loss in the second phase was the main decomposition. In this phase, the main constituents of the composites, i.e., the matrix and fiber (cellulose, hemicellulose, and lignin), were degraded. The third phase was the final phase in the constituent decomposition [38].

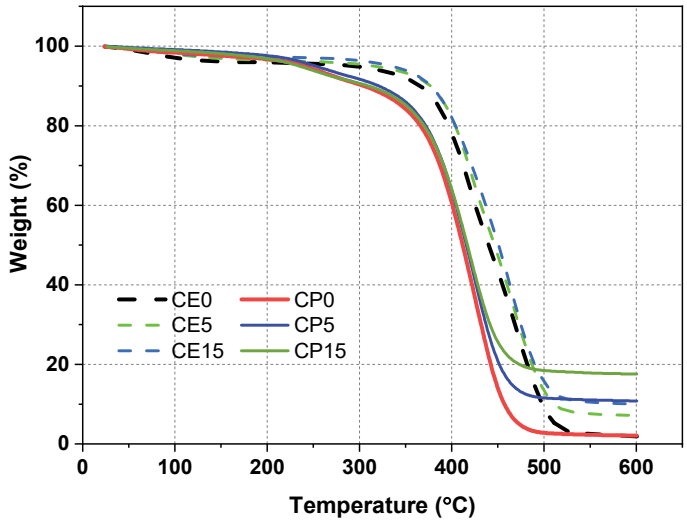

Figure 14: The TGA curves of the Al_2O_3-filled PALF-reinforced composites

Fig. 14 shows that the main decomposition temperature range of the CE0 sample (0% Al_2O_3 loading) was between 382.7 and 505.73 °C. The first peak was between 268 and 442 °C, with a threshold of 418 °C. The second decomposition was between 442 and 540 °C, with a maximum of 469 °C (Fig. 14). The two peaks corresponded to a weight loss of about 79.5%, and the addition of Al_2O_3 to the PALF-reinforced composites had shifted the TGA curve to the right. This finding showed the positive effect of Al_2O_3 on the composites' thermal stability. In the case of the CE5 sample (5 wt% Al_2O_3), the first peak was between 242 and 444 °C, with a maximum of 423 °C, and the last decomposition phase was in the range of 444–540 °C, with a maximum of 469 °C. Furthermore, several mass losses of the CE15 sample (15 wt% Al_2O_3) occurred in the range of 392–540 °C. Derivative Thermogravimetry (DTG) (Fig. 14) showed the main temperature peak of the complicated decomposition of TPU around 467 °C. The decomposition of CE5 and CE15 was very fast, with complicated degradation and weight losses of about 74.4% and 70.5%, respectively.

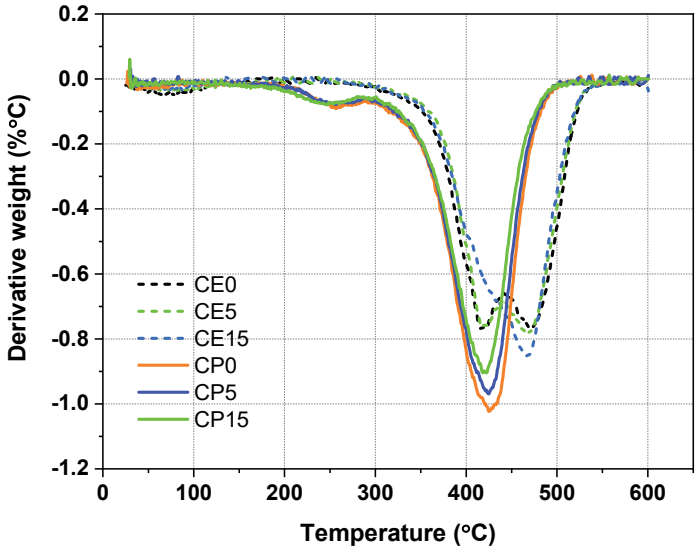

Figure 15: The DTG curve of the Al_2O_3-filled PALF-reinforced composites.

The TGA curve of the composite materials made of PALF and unsaturated polyester resins (UPRs) exhibited a similar behavior to that of the epoxy composites, as shown in Fig. 14. However, the decomposition temperatures of all samples of the UPRs composites were lower than those of the epoxy composites. The decomposition temperatures of CP0, CP5, and CP15 ranged between 363 and 453 °C, 364 and 456 °C, and 365 and 460 °C, respectively, and they were comparatively lower than those of the epoxy composite samples. The CP samples disintegrated rapidly with complicated decomposition in the range of 297–510 °C, with a weight loss of about 59.6 and 67.5%. Furthermore, charcoal residues

were generated from the decomposition that occurred, which was observed at 550 °C. The composites produced charcoal residues in the range from 2.2% to 17.9%, in which case the highest and lowest charcoal residues were produced by CP15 and CE0, respectively. Increasing the amount of alumina filler would increase the amount of charcoal residues. The characteristics of the alumina filler, which has better heat resistance than the fiber and matrix, played an essential role in increasing charcoal residue production.

The DTG curve (Fig. 15) shows the maximum temperature peaks of the complicated decomposition of CP0, CP5, and CP15 at around 421, 424, and 425 °C, respectively. The addition of Al_2O_3 increased the initial temperature of the main decomposition, and the Al_2O_3 microparticles created a char layer and reduced oxidative degradation. The increased amount of Al_2O_3 microparticles in the composites made the process of creating a char layer faster. This phenomenon reduced ignition and resulted in weight loss. This finding demonstrated that the incorporation of Al_2O_3 microparticles increases composites' thermal stability, particularly in terms of the polymer matrix. This result is supported by a previous study [39], which proved that silica positively increases the thermal stability of spruce wood composites.

Conclusions

This research examined the effect of Al_2O_3 microparticles on the physical, mechanical, and thermal stability properties of epoxy and UPRs composites reinforced with PALF. PALF-reinforced composites were made with varying levels of Al_2O_3 content (0, 5, 10, 15% by weight) by hand lay-up. The addition of Al_2O_3 microparticles affected the physical, mechanical, and thermal stability properties of epoxy and UPRs composites reinforced with PALF. The flexural strength, hardness, density, water resistance, and thermal stability gradually increased with the %weight of Al_2O_3 in the composite, while the tensile strength decreased. The PALF-reinforced epoxy composites had higher tensile strength than the PALF-reinforced UPRs composites, while the opposite was true for the flexural strength. The CP15 sample (composed of 30% fiber, UPRs matrix, and 15 wt% Al_2O_3) showed superiority in flexural strength (86.20 MPa), Shore D hardness (81.50), experimental density (1.36 g/cm^3), and water absorption capacity (3.33%), but not in tensile strength. TGA observations of the composites showed that the thermal stability increased with more alumina microparticles added, and the CE15 sample showed higher thermal stability than the other samples. The characterization results showed that alumina-filled PALF-reinforced composites have the potential as engineering materials. However, their application must consider the working loading conditions.

Acknowledgment

The author expresses profound gratitude to the Politeknik Negeri Lhokseumawe, Aceh, Indonesia for the support and funding of this study.

References

[1] Kopparthy, S.D.S., Netravali, A.N. (2021). Green composites for structural applications, Composites Part C: Open Access, 6, pp. 100169, DOI: 10.1016/j.jcomc.2021.100169.

[2] Parameswaranpillai, J., Gopi, J.A., Radoor, S., Dominic, C.D.M., Krishnasamy, S., Deshmukh, K., Hameed, N., Salim, N. V., Sienkiewicz, N. (2022). Turning waste plant fibers into advanced plant fiber reinforced polymer composites: A comprehensive review, Composites Part C: Open Access, pp. 100333, DOI: 10.1016/j.jcomc.2022.100333.

[3] Mishra, T., Mandal, P., Rout, A.K., Sahoo, D. (2022). A state-of-the-art review on potential applications of natural fiber-reinforced polymer composite filled with inorganic nanoparticle, Composites Part C: Open Access, pp. 100298, DOI: 10.1016/j.jcomc.2022.100298.

[4] Asim, M., Abdan, K., Jawaid, M., Nasir, M., Dashtizadeh, Z., Ishak, M.R., Hoque, M.E. (2015). A review on pineapple leaves fiber and its composites, International Journal of Polymer Science, DOI: 10.1155/2015/950567.

[5] World Population Review. World Population Review.(2023). Pineapple Production by Country 2023. Available at: https://worldpopulationreview.com/country-rankings/pineapple-production-by-country.

[6] Todkar, S.S., Patil, S.A. (2019). Review on mechanical properties evaluation of pineapple leaf fiber (PALF) reinforced polymer composites, Composites Part B: Engineering, 174, pp. 106927, DOI: 10.1016/j.compositesb.2019.106927.

[7] Hasanuddin, I., Mawardi, I., Jaya, R.P. (2023). Evaluation of properties of hybrid laminated composites with different fiber layers based on Coir/Al2O3 reinforced composites for structural application, Results in Engineering, pp. 100948, DOI: 10.1016/j.rineng.2023.100948.
[8] Hsissou, R., Seghiri, R., Benzekri, Z., Hilali, M., Rafik, M., Elharfi, A. (2021). Polymer composite materials: A comprehensive review, Composite Structures, 262, pp. 113640, DOI: 10.1016/j.compstruct.2021.113640.
[9] Sugiman, S., Salman, S., Maryudi, M. (2020). Effects of volume fraction on water uptake and tensile properties of epoxy filled with inorganic fillers having different reactivity to water, Materials Today Communications, 24, pp. 101360, DOI: 10.1016/j.mtcomm.2020.101360.
[10] Latief, F.H., Chafidz, A., Junaedi, H., Alfozan, A., Khan, R. (2019). Effect of Alumina Contents on the Physicomechanical Properties of Alumina (Al2O3) Reinforced Polyester Composites, Advances in Polymer Technology, DOI: 10.1155/2019/5173537.
[11] Sathish, S., Kumaresan, K., Prabhu, L., Gokulkumar, S., Karthi, N., Vigneshkumar, N. (2020). Experimental investigation of mechanical and morphological properties of flax fiber reinforced epoxy composites incorporating SiC and Al2O3, Materials Today: Proceedings, 27, pp. 2249–2253, DOI: 10.1016/j.matpr.2019.09.106.
[12] Ferreira, B.T., da Silva, L.J., Panzera, T.H., Santos, J.C., Freire, R.T.S., Scarpa, F. (2019). Sisal-glass hybrid composites reinforced with silica microparticles, Polymer Testing, 74, pp. 57–62, DOI: 10.1016/j.polymertesting.2018.12.026.
[13] Sumesh, K.R., Kavimani, V., Rajeshkumar, G., Indran, S., Saikrishnan, G. (2021). Effect of banana, pineapple and coir fly ash filled with hybrid fiber epoxy based composites for mechanical and morphological study, Journal of Material Cycles and Waste Management, 23, pp. 1277–1288, DOI: 10.1007/s10163-021-01196-6.
[14] Mahesha, C.R., Suprabha, R., Harne, M.S., Galme, S.G., Thorat, S.G., Nagabhooshanam, N., Seikh, A.H., Siddique, M.H., Markos, M. (2022). Nanotitanium Oxide Particles and Jute-Hemp Fiber Hybrid Composites: Evaluate the Mechanical, Water Absorptions, and Morphological Behaviors, Journal of Nanomaterials, DOI: 10.1155/2022/3057293.
[15] Radoor, S., Karayil, J., Rangappa, S.M., Siengchin, S., Parameswaranpillai, J. (2020). A review on the extraction of pineapple, sisal and abaca fibers and their use as reinforcement in polymer matrix, Express Polymer Letters, 14(4), pp. 309–335, DOI: 10.3144/expresspolymlett.2020.27.
[16] Singh, T., Pruncu, C.I., Gangil, B., Singh, V., Fekete, G. (2020). Comparative performance assessment of pineapple and Kevlar fibers based friction composites, Journal of Materials Research and Technology, 9(2), pp. 1491–1499, DOI: 10.1016/j.jmrt.2019.11.074.
[17] Senthilkumar, K., Saba, N., Chandrasekar, M., Jawaid, M., Rajini, N., Alothman, O.Y., Siengchin, S. (2019). Evaluation of mechanical and free vibration properties of the pineapple leaf fiber reinforced polyester composites, Construction and Building Materials, 195, pp. 423–431, DOI: 10.1016/j.conbuildmat.2018.11.081.
[18] Potluri, R. (2019). Mechanical properties of pineapple leaf fiber reinforced epoxy infused with silicon carbide micro particles, Journal of Natural Fibers, 16(1), pp. 137–151, DOI: 10.1080/15440478.2017.1410511.
[19] Faruk, O., Bledski, A.K., Fink, H.P., Sain, M. (2012). Biocomposites reinforced with natural fibers: 2000-2010. Progress in Polymer Science, 37 p. 1552-1596, DOI: 10.1016/j.progpolymsci.2012.04.003.
[20] Fenta Aynalem, G., Sirahbizu, B. (2021). Effect of Al2O3 on the tensile and impact strength of flax/unsaturated polyester composite with emphasis on automobile body applications, Advances in Materials Science and Engineering, pp. 1–9, DOI: 10.1155/2021/6641029.
[21] Abu-Okail, M., Alsaleh, N.A., Farouk, W.M., Elsheikh, A., Abu-Oqail, A., Abdelraouf, Y.A., Ghafaar, M.A. (2021). Effect of dispersion of alumina nanoparticles and graphene nanoplatelets on microstructural and mechanical characteristics of hybrid carbon/glass fibers reinforced polymer composite, Journal of Materials Research and Technology, 14, pp. 2624–2637, DOI: 10.1016/j.jmrt.2021.07.158.
[22] Mawardi, I. (2019). Microfibrillation of Coir Using High Speed Blender to Improvement of Tensile Behavior of Coir Reinforced Epoxy Composites, KnE Engineering, , pp. 157–170, DOI: 10.18502/keg.v1i2.4441.
[23] ASTM D792. (2020). Standard Test Methods for Density and Specific Gravity (Relative Density) of Plastics by Displacement, West Conshohocken, PA, USA, ASTM International.
[24] ASTM D570. (2000). Standard Test Method for Water Absorption of Plastics, West Conshohocken, PA, USA, ASTM International.
[25] ASTM D3039. (2014). Standard Test Method for Tensile Properties of Polymer Matrix Composite Materials, West Conshohocken, PA, USA, ASTM International.
[26] ASTM, D.-03. (2003). Standard Test Methods for Flexural Properties of Unreinforced and Reinforced Plastics and Electrical Insulating Materials, West Conshohocken, PA, USA, American Society for Testing and Materials.
[27] ASTM 2240. (2016). Standard Test Method for Rubber Property—Durometer Hardness, West Conshohocken, PA,

USA, ASTM International.
[28] ASTM E 1131–08. (2010). Standard Test Method for Compositional Analysis by Thermogravimetry, West Conshohocken, PA, USA.
[29] Asim, M., Jawaid, M., Abdan, K., Ishak, M.R. (2016). Effect of alkali and silane treatments on mechanical and fiber-matrix bond strength of kenaf and pineapple leaf fibers, Journal of Bionic Engineering, 13(3), pp. 426–435, DOI: 10.1016/S1672-6529(16)60315-3.
[30] Yazman, Ş., Samancı, A. (2019). A comparative study on the effect of CNT or alumina nanoparticles on the tensile properties of epoxy nanocomposites, Arabian Journal for Science and Engineering, 44, pp. 1353–1363, DOI: 10.1007/s13369-018-3516-4.
[31] Yousri, O.M., Abdellatif, M.H., Bassioni, G. (2018). Effect of Al2O3 Nanoparticles on the Mechanical and Physical Properties of Epoxy Composite, Arabian Journal for Science and Engineering, 43, pp. 1511–1517, DOI: 10.1007/s13369-017-2955-7.
[32] Wu, M., Lu, L., Yu, L., Yu, X., Naito, K., Qu, X., Zhang, Q. (2020). Preparation and characterization of epoxy/alumina nanocomposites, Journal of Nanoscience and Nanotechnology, 20(5), pp. 2964–2970, DOI: 10.1166/jnn.2020.17460.
[33] Wang, Z., Huang, X., Bai, L., Du, R., Liu, Y., Zhang, Y., Zhao, G. (2016). Effect of micro-Al2O3 contents on mechanical property of carbon fiber reinforced epoxy matrix composites, Composites Part B: Engineering, 91, pp. 392–398, DOI: 10.1016/j.compositesb.2016.01.052.
[34] Vinay, S.S., Venkatesh, C. V. (2021). Effect of nano-Al2O3 particles on mechanical and wear behaviour of glass fiber epoxy composites, Materials Today: Proceedings, 46, pp. 9004–9007, DOI: 10.1016/j.matpr.2021.05.378.
[35] Zhang, X., Zheng, J., Fang, H., Zhang, Y., Bai, S., He, G. (2018). Al2O3/graphene reinforced bio-inspired interlocking polyurethane composites with superior mechanical and thermal properties for solid propulsion fuel, Composites Science and Technology, 167, pp. 42–52, DOI: 10.1016/j.compscitech.2018.07.029.
[36] Nayak, S.K., Satapathy, A. (2021). Development and characterization of polymer-based composites filled with micro-sized waste marble dust, Polymers and Polymer Composites, 29(5), pp. 497–508, DOI: 10.1177/09673911209260.
[37] Smooth-On. (2023). Durometer Shore Hardness Scale. Available at: https://www.smooth-on.com/page/durometer-shore-hardness-scale/.
[38] Mawardi, I., Aprilia, S., Faisal, M., Rizal, S. (2021). Characterization of Thermal Bio-Insulation Materials Based on Oil Palm Wood: The Effect of Hybridization and Particle Size, Polymers, 13(19), pp. 3287, DOI: 10.3390/polym13193287.
[39] Bazyar, B., Samariha, A. (2017). Thermal, flammability, and morphological properties of nano-composite from fir wood flour and polypropylene, BioResources, 12(3), pp. 6665–6678, DOI: 10.15376/biores.12.3.6665-6678.